environmental microbiology

Environmental Microbiology (2017) **19**(1), 174–184 doi:10.1111/1462-2920.13551

Diet-induced changes of redox potential underlie compositional shifts in the rumen archaeal community

Nir Friedman,[1,2,3] Eran Shriker,[1,2,3] Ben Gold,[1] Thomer Durman,[1] Raphy Zarecki,[4] Eytan Ruppin[5,6,7] and Itzhak Mizrahi[1]*

[1] *The Department of Life Sciences & the National Institute for Biotechnology in the Negev, Ben-Gurion University of the Negev, Beer-Sheva 84105, Israel.*

[2] *Department of Ruminant Science, Institute of Animal Sciences, Agricultural Research Organization, Volcani Center, P.O. Box 6, Bet Dagan 50250, Israel.*

[3] *The Porter School of Environmental Studies, Tel Aviv University, Tel Aviv, 69978, Israel.*

[4] *Center for Bioinformatics and Computational Biology & Department of Computer Science, Tel Aviv University, Tel Aviv 69978, Israel.*

[5] *The Sackler School of Medicine, Tel Aviv University, Tel Aviv 69978, Israel.*

[6] *Blavatnik School of Computer Sciences, Tel Aviv University, Tel Aviv 69978, Israel.*

[7] *Department of Computer Science and Center for Bioinformatics and Computational Biology, University of Maryland, College Park, MD 20742, USA.*

Summary

Dietary changes are known to affect gut community structure, but questions remain about the mechanisms by which diet induces shifts in microbiome membership. Here, we addressed these questions in the rumen microbiome ecosystem – a complex microbial community that resides in the upper digestive tract of ruminant animals and is responsible for the degradation of the ingested plant material. Our dietary intervention experiments revealed that diet affects the most abundant taxa within the microbiome and that a specific group of methanogenic archaea of the order Methanomicrobiales is highly sensitive to its changes. Using metabolomic analyses together with in vitro microbiology approaches and whole-genome sequencing of *Methanomicrobium mobile*, a key species within this group, we identified that redox potential changes with diet and is the main factor that causes these dietary induced alternations in this taxa's abundance. Our genomic analysis suggests that the redox potential effect stems from a reduced number of anti-reactive oxygen species proteins coded in this taxon's genome. Our study highlights redox potential as a pivotal factor that could serve as a sculpturing force of community assembly within anaerobic gut microbial communities.

Received 23 June, 2016; accepted 26 September, 2016. *For correspondence. E-mail imizrahi@bgu.ac.il

Introduction

The mammalian gut microbiome is now well recognized to play a central role in its host's physiology (Ley *et al*., 2008). Nevertheless, the forces that shape these cardinal microbial communities are still not fully understood. Diet and eating behavior have been shown to play a major role in shaping the gut microbiome of mammals (Muegge *et al*., 2011). Studies in monogastric mammals, such as mice and humans, have shown that dietary changes have a major effect on the gut microbiome, even within a single day after the shift (Faith *et al*., 2011; Walker *et al*., 2011; David *et al*., 2014). In addition, several studies have shown that different dietary regimes have an extensive impact on rumen microbiome composition (Zhou *et al*., 2011; Danielsson *et al*., 2012; Mao *et al*., 2016).

In general, the main sculpting force in diets is thought to be nutrient composition, such as protein versus carbohydrates (Muegge *et al*., 2011; David *et al*., 2014). However, these direct effects do not explain all diet-induced shifts in microbiomes (Davis *et al*., 2011). Therefore, alternative mechanisms are likely to account for some of the changes. Effect of pH has been discussed (Walker *et al*., 2005), but it is likely that this is not the only abiotic factor responsible. Hence, there is a gap in knowledge on the mechanisms that underlie diet-induced changes in microbiomes.

In this study, our aim was to characterize the influence of dietary shift on the rumen microbiome structure as well as to evaluate the parameters generated by microbiome processing of the diet and their effect on microbiome structure and composition. To this end, we monitored individual animals' rumen microbiomes with dietary shifts; we examined the taxonomic and metabolomic composition, as well as the physical parameters of the rumen fluids resulting from the processing of different diets by the microbiome.

We then measured the causal role of these parameters in inducing shifts of specific organisms that were responsive to diet, as well as on their gene composition.

We show that the dietary effect on the rumen microbiome affects mainly the most abundant members of the microbiome. Combining metabolomic analysis of the rumen fluids with *in vitro* microbiology experiments, we found that out of the many parameters that change with dietary shift, redox potential, a physical factor of the rumen fluids, has a marked effect on a specific, highly diet-responsive methanogenic order. Using genome analysis, we discovered genomic features that can explain the examined methanogen diet related shift. Our findings identify redox potential as a mechanism by which diet could impact gut microbiome composition.

Results

Diet impacts the most abundant organisms of the rumen microbiome

We first explored the effect of diet on the rumen microbiome structure. To this end, we introduced two diets consisting of different grain ratios (Supporting Information Table S1) – 65% grain (high-grain) and 0% grain (non-grain). In order to isolate microbiome components that are consistent with dietary change and not influenced by time related factors, we conducted two independent experiments 6 months apart from each other. To eliminate other environmental factors, the introduction order of the diets was changed in the two experiments: in the first, the high-grain diet was introduced first and in the second, the non-grain diet was first. Each group of animals was fed both diets for approximately 1 month (Supporting Information Fig. S1). In addition, in the second experiment, two animals were kept on the same diet throughout the experiment as a control (Supporting Information Fig. S1).

In order to understand the effect of dietary shift on microbiome structure, we identified sensitive taxa that were present in all samples coming from one diet and decreased to undetectable amounts in all samples with the diet shift. These 'diet-unique operational taxonomic units (OTUs)', were then plotted on a rank abundance curve (Whittaker plot) in order to localize them on the overall microbiome structure (Fig. 1A). Interestingly, these diet-unique OTUs belonged to the most abundant members of the microbiome within the applied diet (Fig. 1A). We further explored the identity of the diet-responsive taxa to determine whether the dietary effect is limited to a defined phylogenetic group or has a broader effect on a wide range of taxonomic groups. Our analysis showed that diet change affects a broad spectrum of OTUs belonging to a wide range of phylogenetic groups – 11 phyla for the non-grain diet and 8 for the high-grain diet (Fig. 1B).

Dietary change has been previously reported to affect rumen microbial communities, but information on how this effect stands with regard to individual variability is still lacking.

Nonmetric multidimensional scaling (NMDS) and cluster analyses of the sequenced 16S rRNA amplicons from the two diets revealed that the dietary effect on the rumen microbiome is stronger than individual variability as the samples clustered together according to diet and not according to the animals from which they were collected. This was also true even when animals from the two experiments were plotted on the same ordination (Fig. 1C and D). Moreover, the order in which the diets were introduced did not alter the dietary effect on the microbiome, further stressing the strength of this effect on the rumen microbiome.

The methanogenic archaeal community is highly responsive to diet change

Interestingly, out of the four methanogenic archaeal orders detected in our samples, two – the Methanomicrobiales and Methanosarcinales, included identified diet-unique OTUs (Fig. 2A, upper blue panel). Each order was represented by a single genus: *Methanomicrobium* for the Methanomicrobiales and *Methanomicrococcus* for the Methanosarcinales (Fig. 2A, lower green panel). These orders exhibited the pattern of the diet-unique OTUs as they were completely absent from all high-grain diet samples and were detected in all non-grain diet samples (Fig. 2). Taxonomic assignments of these OTUs revealed that the *Methanomicrobium* related species was 99% identical to *Methanomicrobium mobile* strain BP. No further annotation for the *Methanomicrococcus* OTU was found. Two more bacterial orders showed the same pattern of complete absence from high-grain diet and exclusively present in non-grain diet, nevertheless these could be only annotated at the phylum level as members of Elusimicrobia.

Although our sequencing results showed a clear difference in methanogenic community compositions between the two diets, they provided little insight into the kinetics of these changes during the experiment. Hence, we monitored the kinetics of these orders' abundance over time using a quantitative real-time PCR (qRT-PCR) analysis specifically targeting these methanogenic orders as well as two other methanogenic orders and the overall archaeal domain (Yu *et al*., 2005). The total archaeal domain did not show any significant changes between the two diets during the experiment. However, we observed a sharp increase in the abundance of Methanomicrobiales and a moderate decrease in the abundance of Methanobacteriales coinciding with the dietary switch, regardless of the applied order of the diets (Fig. 2B and Supporting Information Fig. S2), further supporting our previous finding regarding the

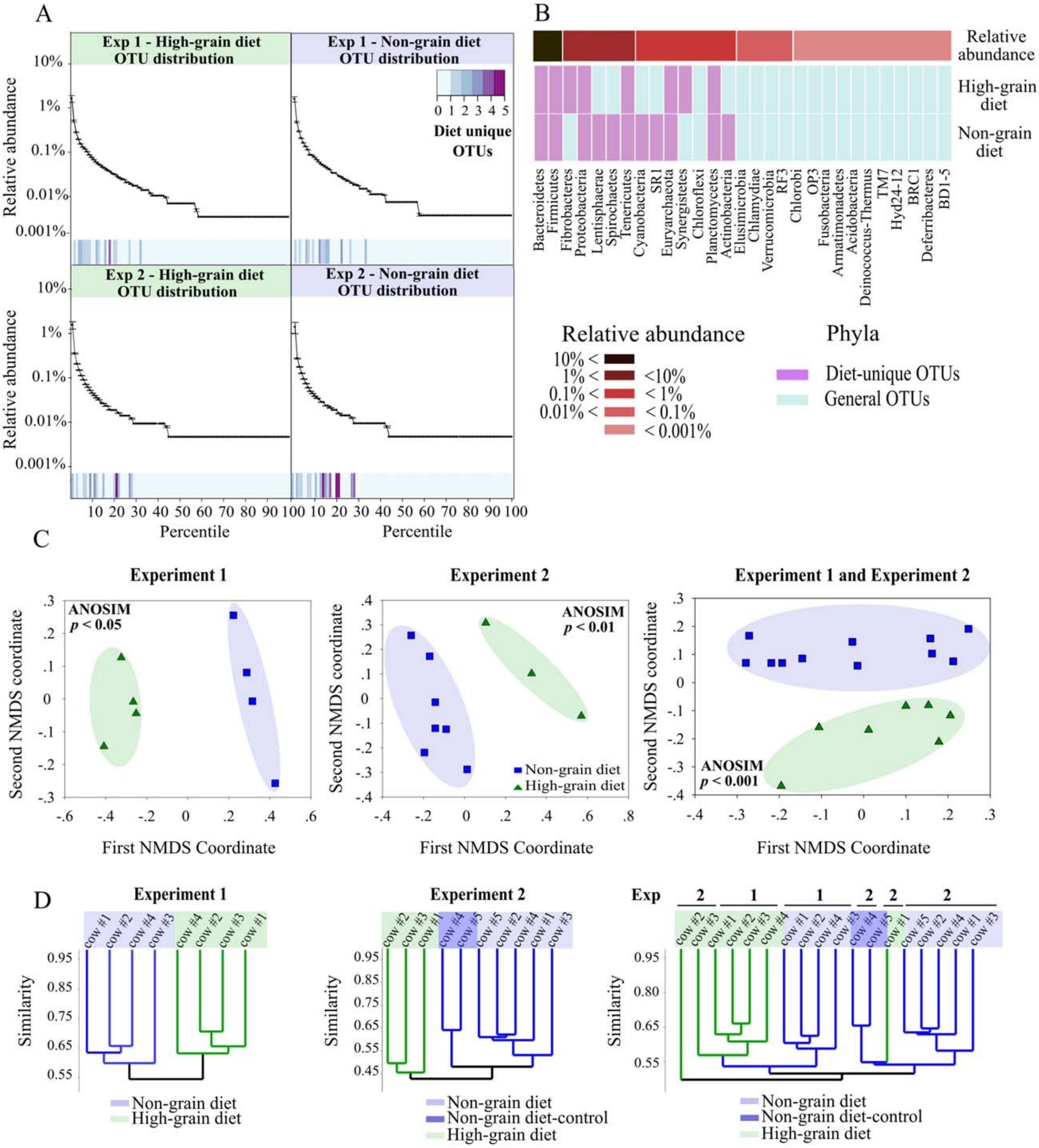

Fig. 1. Diet affects structure and composition of the rumen microbiome at the most prevalent members.
Amplicon 16S rRNA sequencing analysis of two independent diet-shift experiments. Samples extracted from the rumen microbiome under the non-grain diet are denoted in blue and those from the microbiome under the high-grain diet are denoted in green.
A. Principal component analysis of OTUs from the two diets.
B. Hierarchical clustering analysis using Bray Curtis similarity metric of OTUs from the two diets.
C. Rank abundance curve (Whittaker plot) of all OTUs divided into percentiles was created for the two dietary regimes in each experiment. Unique OTUs that are present in all animals in one diet and completely absent from all animals after the diet shift were plotted as a heat map corresponding to relevant percentiles, where darker purple colors denote more OTUs in a given percentile. The *Y* axis represents the average relative abundance of each percentile and the *X* axis represents the percentiles.
D. Heat map representation of phylum association of diet-unique OTUs according to their relative abundance. Along the upper bar, shades of red represent the average relative abundance of each specific phylum of the rumen microbiome. On the heat map, phyla in which diet-unique OTUs are included are denoted in purple and phyla that do not include diet-unique OTUs (general OTUs) are in light blue. [Colour figure can be viewed at wileyonlinelibrary.com]

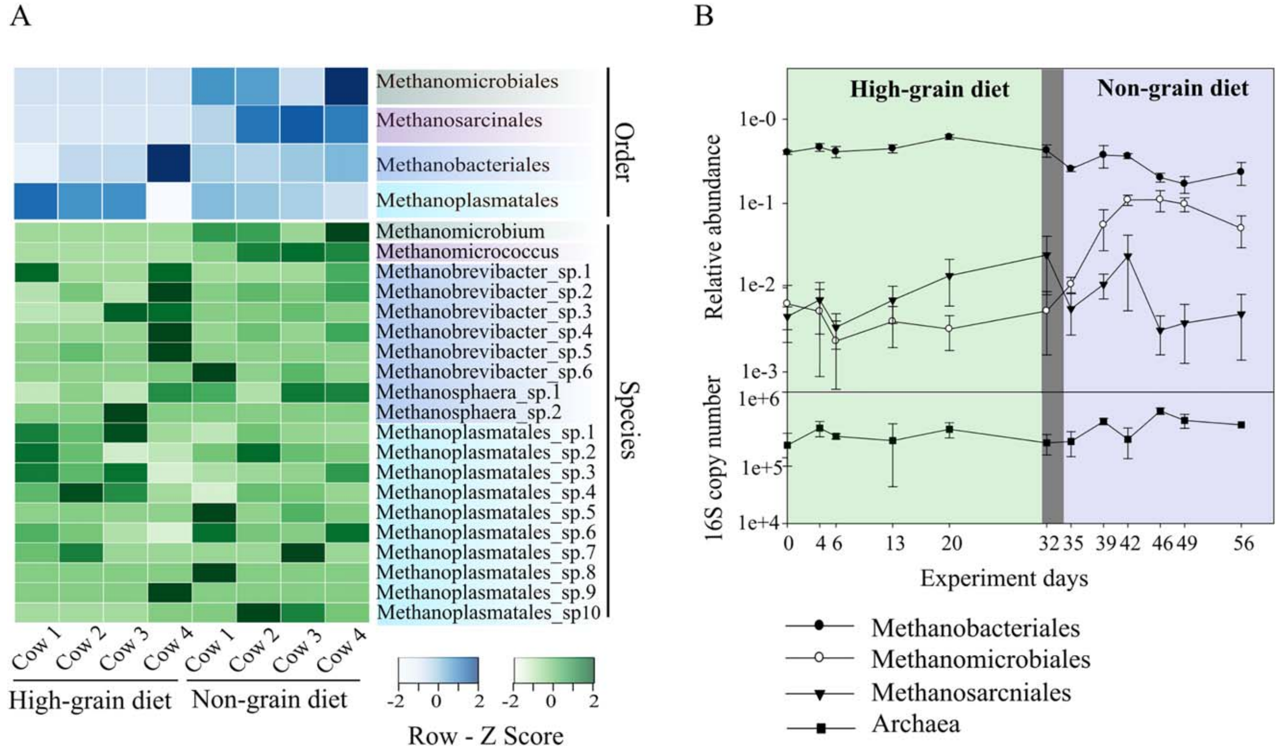

Fig. 2. Diet strongly impacts archaeal methanogenic community composition.
A. Heat map analysis of OTUs corresponding to methanogenic archaea under non-grain and high-grain diets. Community composition at the order level is represented in the upper panel in blue shades and at the species level in the lower panel in green shades. The order-level association of methanogenic species is denoted by the color coding of the taxonomic annotation on the right, corresponding to the same color at the order level. The sample associations are presented below the heat map.
B. Real-time qPCR of the three major methanogenic orders—Methanobacteriales, Methanomicrobiales, Methanosarcinales—and of total archaea. DNA from rumen samples was extracted and subjected to qRT-PCR analysis. Days 1–31 represent the high-grain diet (light green background), days 32–34 represent the 3-day habituation period to the new diet (dark gray background) and days 35–56 represent the non-grain diet (light purple background). Each day represents the average of four cows. The *X* axis represents the days of the experiment. The *Y* axis of the upper panel represents the proportion of each methanogen order out of total archaea. The *Y* axis in the lower panel represents the absolute copy number of archaeal 16S rRNA. Mean for each time point is plotted ± SEM. [Colour figure can be viewed at wileyonlinelibrary.com]

deterministic effects of diet. These reciprocal changes of the Methanomicrobiales and Methanobacteriales orders were highly correlated (Spearman's rank correlation coefficient; experiment 1: $R = -0.86$, $p < 0.001$; experiment 2: $R = -0.67$, $p < 0.001$). In this analysis the order Methanosarcinales did not show any change in abundance as a function of diet change which was inconsistent with the 16S rRNA amplicon sequencing analysis. This inconsistency could potentially result from different specificity of the primer sets used in the qRT-PCR and the16S rRNA amplicon sequencing. We therefore focused on understanding diet-related changes in the Methanomicrobiales and Methanobacteriales in which agreement between the two methods was observed.

A negative correlation between these two orders as a function of diet change suggested that they may compete for the same ecological niche, and that the diet change affects the fitness of one or both of them in an opposite manner, thereby enabling occupation of the niche when the diet shift is applied. To test this hypothesis, we set out to examine it *in vitro* with previously isolated methanogens. This enabled us to experimentally examine the effect of diet on these organisms, answering our questions regarding niche partitioning between the different methanogenic orders as a function of diet.

Methanomicrobiales order represented by Methanomicrobium mobile is specifically affected by redox potential of the rumen fluids

Representation of the Methanomicrobiales by a single OTU closely related to *M. mobile* presented the opportunity to explore the diet effect on this organism. First, we set out to understand the absence of *M. mobile* from the high-grain diet and its growth in the non-grain diet. We specifically aimed to distinguish between two possible scenarios: the first involving the effect of the host animal and direct interactions with other members of the microbiome and the second involving the composition of the rumen fluids resulting from microbiome processing of the high-grain diet. To this end, we grew *M. mobile in vitro* in sterile rumen fluids originating from animals fed on each of these diets. *M. mobile* could only grow with the non-grain diet, as observed in our qRT-PCR analysis and methane measurements (Fig. 3A). These findings highlighted rumen fluids composition as the more feasible explanation for the *in vivo* observations.

As our results suggested that physical or chemical factors within the rumen fluids affect *M. mobile* growth, we analyzed the physical characteristics and metabolomic content of the rumen fluids derived from the two different diets. Whereas the rumen fluids derived from the non-grain diet contained more amino acids, the rumen fluids from the high-grain diet contained more carbohydrates in the form of simple sugars. Furthermore, significantly lower redox potential and higher pH were observed in the non-grain diet rumen fluids (Fig. 3B–D).

To further decipher which components of the rumen fluids affect *M. mobile* growth, we equilibrated each of the differentiating factors separately in the high-grain diet and non-grain diet rumen fluids. The strongest effect on *M. mobile* growth occurred when the redox potential was decreased. Increasing pH levels (6.8–7) and thus imitating the pH levels observed in non-grain diet, also promoted *M. mobile* growth, but to a much lesser extent, and amino acid and vitamin additions had even weaker effects (Fig. 4A).

The strong response of the Methanomicrobiales, represented by *M. mobile*, to redox potential led us to ask whether this could explain the negative correlation observed *in vivo* between the Methanomicrobiales and Methanobacteriales. Specifically, we explored whether this phenomenon is due to an opposite effect of diet on these orders or whether only the Methanomicrobiales are negatively affected by the diet change, while members of the Methanobacteriales occupy this ecological niche. Our results suggested the latter. Members of the Methanobacteriales did not exhibit differential growth in the high-grain rumen fluids, with or without the addition of a reducing agent under controlled pH conditions, whereas the Methanomicrobiales, represented by *M. mobile*, showed an up to 3000-fold increase in growth with supplementation of a reducing agent (Fig. 4B).

Redox sensitivity is explained by a reduced repertoire of anti-reactive oxygen species genes in M. mobile

We sequenced and analyzed the genome of *M. mobile* (DSM 1539) to explore whether its genetic repertoire could explain its unique redox sensitivity. The draft genome was assembled into six contigs with a total of 1 690 000 bp containing 1650 predicted open reading frames (ORFs). When we performed a genome comparison of *M. mobile* and 12 other methanogens that belong to the three main orders present in the rumen we found that *M. mobile* had the lowest number of anti-reactive oxygen species (ROS) proteins of all of the methanogens examined (Fig. 5).

Discussion

Our aim in this study was to understand the effects of dietary shift on rumen microbial community structure, as well as the forces that drive these effects. We used two diets with extreme differences in grain content and introduced them in a changing order (Supporting Information Fig. S1). We found that community assembly with respect to diet change is a superior force to individual variability and time effect, giving rise to very similar microbial communities regardless of the sequence in which the diets are applied. This was observed when the overall community was examined using 16S rRNA amplicon sequencing data (Fig. 1A), as well as when we examined specific methanogenic orders using qRT-PCR (Fig. 2B). In ruminants, the rumen is the first gastrointestinal compartment to be exposed to diet after ingestion. This is in contrast to the colon microbiomes usually studied in monogastric animals, which are sampled after being exposed to the entire digestive tract, as it is positioned in its last part. Therefore, in the ruminant microbiomes the diet's effect is potentially more enhanced. This point was emphasized in a recent study where the effect of diet was greater than host and geography in 742 single microbiome samples of ruminant and camelid animals that were collected in 35 countries, (Henderson *et al*., 2015). Interestingly, some diet-unique OTUs that could not be detected in one diet increased to high abundance when the diet was changed (Fig. 2). This finding indicates the plasticity of the microbiome structure, which recovered when conditions were retrieved. This is congruent with previous studies examining alterations in the human microbiome as a function of diet shift, where the occurrence of dominant bacterial groups after a dietary shift was rapidly reversed by the subsequent diet (Walker *et al*., 2011; David *et al*., 2014).

With regard to community structure, we showed that a relatively small number of taxa that are highly abundant and span a vast number of phylogenetic groups are most affected by the diet change (Fig. 1A and B). This might be because these organisms are best suited to the rumen ecological niche under a specific dietary regime; once the diet changes and new ecological niches, together with selective forces, are introduced, these organisms are outcompeted by a few new and better adapted organisms that occupy and dominate this new niche. To the best of our knowledge, this is the first time that this effect on rumen community structure has been described and it is tempting to speculate that this observation holds true whenever a change in selective pressure is applied.

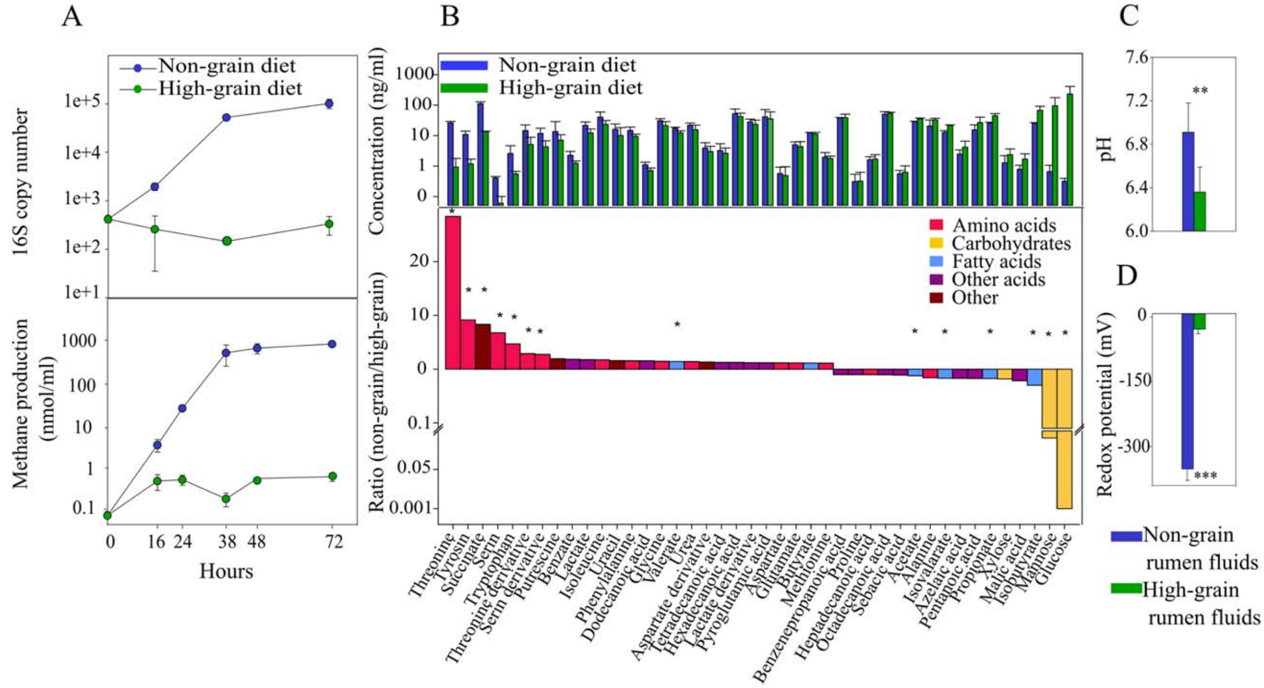

Fig. 3. Microbial responsiveness to diet change is recapitulated *in vitro* by inoculation in diet derived rumen fluids having different physical and metabolomic characteristics.
A. *M. mobile* was grown in sterile non-grain and high-grain-derived rumen fluids. The 16S rRNA gene copy number of *M. mobile* was monitored by qRT-PCR analysis (upper panel) and methane gas was monitored using GC by sampling the tube headspace (lower panel). The *X* axis represents the sampling time points. The *Y* axis in the lower panel represents the amount of methane production and in the upper panel, the *M. mobile* 16S rRNA copy number. For each time point, the mean of three independent experiments and SEM are plotted.
B. GC and GC–MS analyses of non-grain and high-grain-derived rumen fluids. The upper panel represents the absolute concentration of each metabolite. Each bar represents the mean ± SEM of at least two biological repeats and two technical repeats. The lower panel represents the concentration ratio between the non-grain and high-grain-derived rumen fluids. Asterisks represent significant differences (*t*-test, $p < 0.05$) between the metabolite concentrations in the two diets.
C. pH measurement for the two diets. Each bar represents an average of triplicate measurements.
D. Redox potential measurements for the two diets. Each bar represents an average of triplicate measurements. [Colour figure can be viewed at wileyonlinelibrary.com]

To understand the mechanisms behind these diet-derived changes, we turned to *in vitro* experiments with cultivable microorganisms. Interestingly, an archaeal order represented by a single cultivable OTU annotated as *M. mobile* was found uniquely under the non-grain diet. Using a metabolomic approach together with other physical measurements of the rumen fluids derived from the different diets, we found that redox potential has the most prominent effect on *M. mobile*; this effect was specific to *M. mobile* and had little or no effect on other examined methanogens (Fig. 4B). This experiment recapitulated the *in vivo* observations and answered our questions about the negative correlation between the Methanomicrobiales and Methanobacteriales with regard to dietary change (Fig. 2B). These findings suggested that the negative correlation stems from the niche's occupation by the Methanobacteriales, following exclusion of the Methanomicrobiales due to selection driven by higher redox potential. When we examined the genome of *M. mobile* we found lower presence of anti-ROS genes compared to other examined methanogen genomes that could suggest its sensitivity to higher redox potential (Fig. 5).

Redox potential has been shown to play a cardinal role in shaping microbial communities in oxygen minimum zones of oceans where niche partitioning as a function of redox potential gradients shapes the microbes' metabolic networks (Wright *et al*., 2012). Redox potential in the gut is known to change from high to low values early in the lives of ruminant animals as well as humans, where it has a marked effect on the microbiome structure (Lozupone *et al*., 2012; Jami *et al*., 2013). Redox potential is not usually measured during experiments performed in the context of diet and gut microbiomes. However, in several studies of monogastric and ruminant animals, redox potential has been shown to change with diet (Jonas *et al*., 1999; Feillet-Coudray *et al*., 2009; Liu *et al*., 2009; Xiao *et al*., 2010). Specifically in ruiminants, and consistent with our findings, redox potential tended to be lower (45–100 mV) in animals

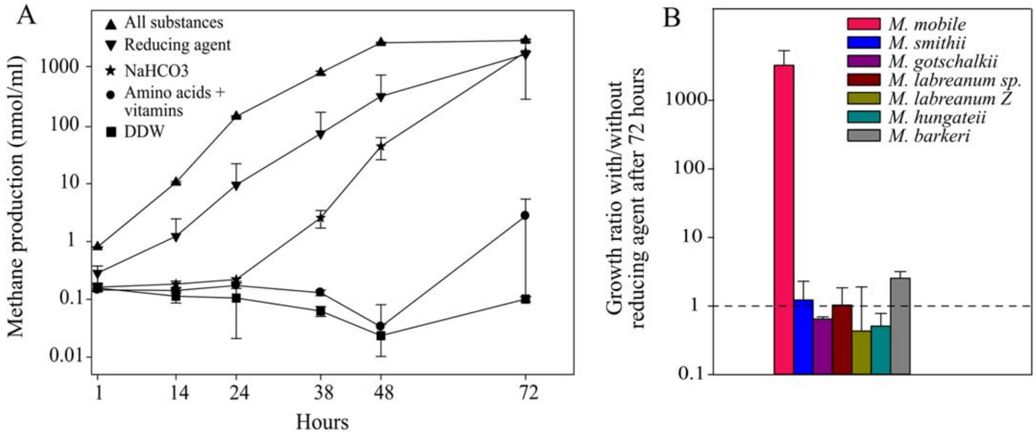

Fig. 4. Redox Potential change explains diet derived differential growth of key methanogen.
A. Growth of *M. mobile* in high-grain-derived rumen fluids supplemented with one of the following substances: DDW, amino acids and vitamins, $NaHCO_3$, reducing agent (cysteine-HCl) or all of the substances together. The *X* axis represents the sampling time points and the *Y* axis represents methane production as measured by GC.
B. Growth ratio based on methane production of *M. mobile* and six other methanogens with or without the addition of reducing agent.The *Y* axis represents the ratio of growth with to growth without reducing agent after 72 h. [Colour figure can be viewed at wileyonlinelibrary.com]

fed low-grain diet compare to animals fed high-grain diet (Barry *et al*., 1977; Marounek *et al*., 1982a; Daniel *et al*., 2010). The cause for this change is not entirely clear: it could originate directly from the diet and its additives, or from metabolic activities performed by the microbiome members, which in turn reshape the community. Such an explanation could relate to the lower rumen pH in the high-grain diet. This diet is rich in starch, which is quickly

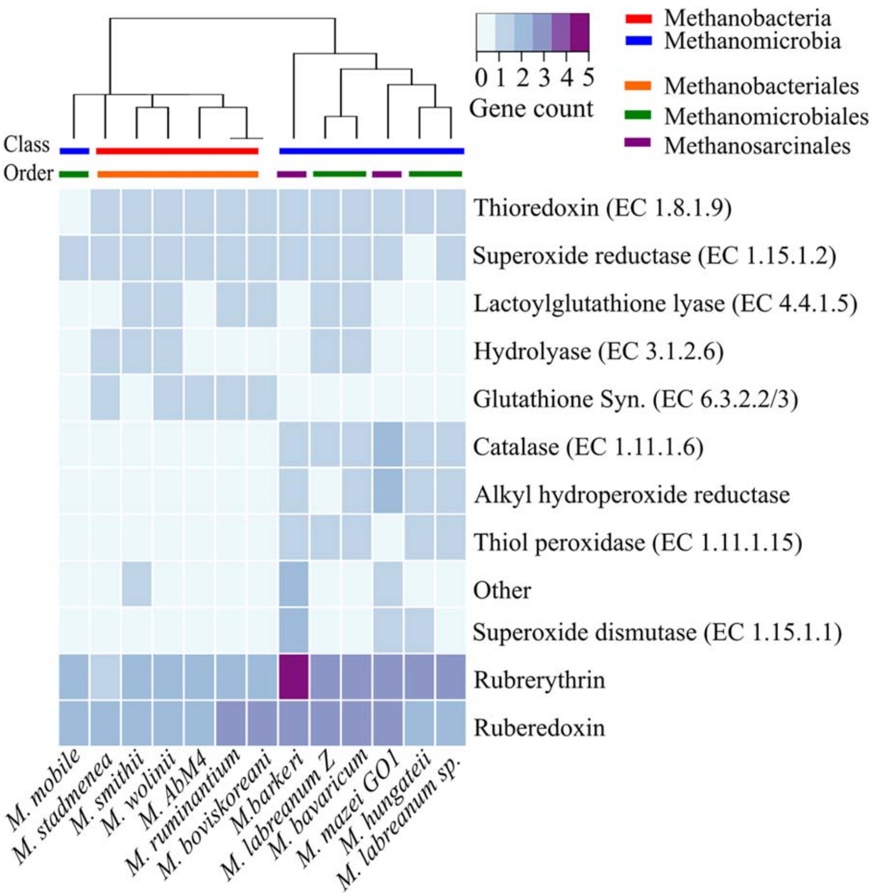

Fig. 5. Oxidative stress enzymes and anti-ROS reactions are underrepresented in *M. mobile* genome.
Genomic comparison of *M. mobile* and 12 other methanogens. Heat map representation of anti-ROS protein number in each methanogen genome. [Colour figure can be viewed at wileyonlinelibrary.com]

fermented by the rumen microbiome therefore causing accumulation of volatile fatty acids (VFAs) that consequently lower the rumen pH (Shaver, 1997). This decrease in rumen pH could elevate redox potential due to the inherent dependence of pH and redox potential on proton-coupled redox reactions (Krishtalik, 2003). Indeed, several studies demonstrated such a relationship in the rumen environment, where a decrease in pH was associated with an increase in redox potential (Marounek *et al*., 1982b; Marounek *et al*., 1987). In our experimental system, we aimed in separating redox potential from pH effect. To that end we used electron-transfer that is not accompanied by proton transfer, therefore changing redox potential without affecting the pH and measuring its direct effect on the examined organisms.

Based on our findings and the immense importance of redox potential in anaerobic environments, we propose that redox potential is a fluctuating diet-derived factor, defining ecological niches that in turn give rise to specialized microorganisms. This discovery may hold high importance not just for ruminants and archaeal communities within them, but also for the human gut microbiota, where facultative anaerobes that benefit from high redox state are typically pathogens or pro-inflammatory species. Taking this parameter into account could potentially enable us to improve cultivation capabilities of anaerobic gut microbes, as well as to manipulate and design gut microbial communities in the future.

Experimental procedures

Animal handling and rumen sampling

All of the experimental procedures described in this study were approved by the Faculty Animal Policy and Welfare Committee of the Agricultural Research Organization (ARO), approval number IL-326/11, and were in accordance with the guidelines of the Israel Council for Animal Care. Cannulated Holstein-Friesian cows were housed at the ARO's experimental dairy farm in Bet Dagan, Israel. The cows were fed the diets described in Supporting Information Table S1 with free access to water. Samples were taken 6 h after feeding as follows: 200 ml ruminal contents were collected via the cow's cannula and filtered through eight layers of cheesecloth to eliminate rumen sediments and large ration particles. The pH was determined immediately by pH meter (IQ Scientific Instruments). The rumen fluids samples were promptly stored after collection at −20°C until further treatment.

Isolation of microbial fraction and DNA extraction from rumen samples

Rumen fluids (50 ml) was homogenized in a blender and centrifuged at 10 000 *g* for 10 min. The pellet was then suspended in extraction buffer (100 mM Tris-HCl, 10 mM EDTA, 150 mM NaCl pH 8.0, 0.15% v/v Tween-80) and incubated for 1 h at 4°C, to detach particle-associated microorganisms from the rumen content. Following slow centrifugation (500 *g*) for 15 min at 4°C, the microbiota-containing supernatant was refiltered through eight layers of cheesecloth, centrifuged at 6000 *g* for 10 min and resuspended in extraction buffer. The pellets were kept at −20°C until DNA extraction, which was performed as described by (Yu and Morrison, 2004) with a few modifications. Briefly, the microbial cells were lysed using bead disruption and lysis buffer [500 mM NaCl, 50 mM Tris-HCl pH 8.0, 50 mM EDTA, 4% v/v sodium dodecyl sulfate (SDS)]. The final supernatant was precipitated using ammonium acetate and isopropanol. The precipitate was then dissolved in TE buffer (10 mM Tris-HCl pH 7.5, 1 mM EDTA pH 8.0), checked for DNA concentration, diluted to 10 ng/μl and stored at −20°C.

Quantitative real-time PCR

A qRT-PCR analysis was performed to investigate the relative abundance of specific methanogen orders through amplification of their 16S rRNA gene. TaqMan probes and primers were used as described elsewhere (Yu *et al*., 2005). A standard curve was generated for the methanogen orders and total archaea by amplifying serial 10-fold dilutions of gel-extracted PCR products obtained by the amplification of each amplicon. The standard curves consisted of four to six dilution points, and were calculated using Rotorgene 6000 series software (Qiagen). Subsequent quantifications were calculated with the same program using the standard curve generated in each run, and one known purified product diluted for the standard curves was added to each quantification reaction to assess its reproducibility. All obtained standard curves met the required standards of efficiency ($R^2 > 0.99$, E > 90%). Reactions were performed in a 10-μl reaction mixture containing 5 μl 2X Sensi fast probe Hi Rox Mix (Bioline, London, UK), 0.5 μl of each primer (500 nM final concentration), 1 μl probe (200 nM final concentration), 1 μl double-distilled water (DDW) and 2 μl of 10 ng/μl DNA template. Amplification consisted of 1 cycle at 95°C for 5 min for initial denaturation and activation of the polymerase system, and then 45 cycles at 95°C for 10 s followed by annealing for 45 s at 60°C for archaea and Methanobacteriales primers, 62°C for Methanosarcinales primers and 63°C for Methanomicrobiales primers, and extension at 72°C for 20 s.

16S rRNA gene sequencing and M. mobile genomic sequencing and analysis

Amplification of the 16S rRNA of the ruminal samples was performed according to (Caporaso *et al*., 2012). The pooled sample was sequenced on the Illumina MiSeq platform according to published protocols (Caporaso *et al*., 2012). Analyses were mostly performed using the Quantitative Insights into Microbial Ecology (QIIME) pipeline package (Caporaso *et al*., 2010). Raw reads were assigned to their designated rumen sample using the split_library.py script. The degree of similarity between sequences was defined as ≥97% to obtain an OTU identity that is commonly considered species level (Muegge *et al*., 2011) and annotated using BLAST against the Silva_111 (Quast *et al*., 2013). OTUs that clustered only one or two reads were manually removed. In total, we characterized 847624 16S rRNA quality reads for 18 samples, an average of 94 603 ± 8134 quality reads per sample for experiment 1 and an average of 9080 ± 1376 quality reads per sample for experiment 2. Analysis of 16S rRNA data was performed using PAST software. *M. mobile* genome sequencing was performed according to the Illumina 'TruSeq DNA PCR-FREE Sample Preparation Guide' low sample (LS) protocol. Assembly of sequenced reads was performed by Velvet assembly tool (Zerbino and Birney, 2008). In total, ~1.75 Mbp in 6 contigs were generated and analyzed as described in the results section.

Statistical analysis

In general, significance was calculated according to paired Student's *t*-test or ANOSIM tests. In all analyses, significance was set at $p < 0.05$ unless otherwise stated. Principal component analysis for high-grain and non-grain diets for both experiments was performed using PAST software (Hammer, 2000).

Strains and growth media

Methanomicrobium mobile (DSM 1519), *Methanobrevibacter smithii* (DSM 861), *Methanobrevibacter gottschalkii* (DSM 11977), *Methanobrevibacter ruminantium* (DSM 1093), *Methanospirillum hungatei* (DSM 864), *Methanocorpusculum labreanum* strain Z (DSM 4855) and *Methanosarcina barkeri* (DSM 800) were purchased from the German collection of microorganisms and cell cultures (DSMZ) and stored in 25% glycerol at −80°C until use. *Methanocorpusculum labreanum sp*. was isolated in our laboratory and kept under the same conditions.

In vitro *growth assays*

To isolate the variables that might affect *M. mobile* growth, rumen fluids after feeding with non-grain and high-grain diets were anaerobically sterilized using a 0.22-μm filter. A 5- to 10-day *M. mobile* culture was concentrated to an OD_{600} of 0.3 and then diluted 1:100 into each of these fluids in duplicate in designated anaerobic (Hungate) tubes. Following inoculation, the samples were pressurized with 2 atmospheres of 80%/20% H_2/CO_2 and kept under continual 110 rpm rotation in the dark. At each time point, headspace gas was monitored by gas chromatography (GC) (as described further on) and DNA was extracted from the samples followed by RT-PCR analysis with archaeal primers as discussed previously.

In another experiment, duplicate samples of sodium bicarbonate (2 g/l), cysteine-HCl (0.5 g/l), yeast extract (0.3 g/l) or DDW were added to rumen fluids from the high-grain diet containing a 1:100 dilution from OD_{600} of 0.3 of *M. mobile*, to examine their ability to restore *M. mobile* growth. Following inoculation, the samples were pressurized with 2 atmospheres of 80%/20% H_2/CO_2 and kept under continual 110 rpm rotation in the dark. Growth was monitored by methane production in the headspace using GC.

Analytical measurements for the diets

GC/GC–mass spectrometry

All metabolites other than the volatile fatty acids (VFAs) were detected and analyzed using GC–MS (mass spectrometry) as described elsewhere (Saleem *et al*., 2013). Briefly, rumen fluids (2 ml) were centrifuged and filtered through a 0.45 μm nonpyrogenic filter (EMD Millipore). All rumen fluids samples were handled immediately and kept at 4°C to minimize any further metabolite degradation.

Ribitol (2 μl) in water (20 μg/ml) was added to a 98-μl sample as a quantification standard to obtain a 100-μl sample. The samples were then loaded with 800 μl of cold HPLC-grade methanol:DDW (8:1 v/v) and vortexed for 1 min. The samples were kept at 4°C for 20 min and then centrifuged at 3800 *g* for 8 min. After centrifugation, 200 μl of the supernatant was evaporated to dryness using a Speedvac concentrator. After evaporation, 40 μl of 20 mg/ml methoxyamine hydrochloride (Sigma-Aldrich) in ACS-grade pyridine was added to the extracted residue and incubated at room temperature for 16 h. After methoximation, 50 μl of N-methyl-N-trifluoroacetamide (MSTFA) with 1% trimethylchlorosilane (TMCS) derivatization agent (Sigma-Aldrich) was added followed by incubation at 37°C for 1 h.

Samples were vortexed after incubation to ensure complete dissolution. Derivatized extracts were analyzed using an Agilent 5975C GC and an Agilent 7890A MS operating in electron impact (EI) ionization mode. Aliquots (1 μl) were injected (splitless) into a 30 m × 0.25 mm × 0.25 μm HP-5MS Ultra Inert column (Agilent Technologies) with helium carrier gas set to a flow rate of 1 ml/min and initial oven temperature of 70°C. The oven temperature was held at 70°C for 2 min, then increased at 10°C/min to a final temperature of 310°C, and a final run time of 45 min. Samples were run using full scan in a mass range of 50–500 m/z (1.7 scans/s) with a detection delay of 4 min. Retention indices were calculated using a C8–C20 alkane standard mixture solution (Sigma-Aldrich) as the external standard. Quantification and identification of trimethylsilylated metabolites were performed using the NIST database and HPLC-grade standards. VFAs were analyzed and quantified by Agilent 7890B GC with a FID detector. Non- and high-grain rumen fluids (1 ml) were centrifuged for 15 min at 16 000 *g* and the pellet was discarded. Rumen fluids (400 μl) was mixed with 100 μl of 25% metaphosphoric acid solution in a 1.5-ml Eppendorf tube. Each sample was immediately vortexed for 1 min then left to stand for 30 min at 4°C. The samples were then centrifuged for 15 min at 11 000 *g* at 4°C. The samples were transferred into a new 1.5-ml Eppendorf tube and

250 μl of methyl tert-butyl ether (MTBE) was added to each sample separately. The samples were then vortexed for 30 s and centrifuged for 1 min at 10 000 *g* at 4°C. The upper phase containing MTBE with VFAs was decanted into a GC vial. Aliquots (1 μl) were injected with a split ratio of 1:25 into a 30 m × 0.32 mm × 0.25 μm ZB-FFAP column (ZEBRON) with helium carrier gas set to a flow rate of 2.4 ml/min and initial oven temperature of 100°C. The temperatures at the inlet and detector were set at 250°C and 300°C, respectively. The oven temperature was held at 100°C for 5 min, then increased at 10°C/min to a final temperature of 125°C and a final run time of 12.5 min. Quantification and identification of metabolites were performed using HPLC-grade standards.

Redox potential

Redox potential was measured by Sartorius pb-11 using a VWR rd-223 ORP electrode. All measurements were performed inside an anaerobic chamber (Coy Industries, Inc.) under anaerobic conditions.

Methanogens genomic analysis

Methanogen genomes were downloaded from NCBI database and uploaded to the 'Rapid Annotation Using Subsystem Technology' (RAST) platform (Aziz *et al*., 2008). Anti-ROS proteins from these genomes were counted and analyzed.

Acknowledgment

The research described here was supported by grants from the Israel Science Foundation (No. 1313/13), by the European Research Council under the European Union's Horizon 2020 research and innovation program (grant agreement No 640384) and by ICA grant 713 02-15-08a.

Data deposition

16S rRNA gene sequencing reads were deposited in the MG-RAST server under IDs 282699 and 282706.

Author contributions

N.F. designed and conducted the experiments, analyses and wrote the paper, E.S. conducted the experiments and analyses, B.G conducted the experiments, T.D. conducted the experiments, R.Z. conducted the analyses, E.R. provided general professional consultation, and I.M. designed the experiments, conducted analyses and wrote the paper.

References

Aziz, R.K., Bartels, D., Best, A.A., DeJongh, M., Disz, T., Edwards, R.A., *et al*. (2008) The RAST Server: rapid annotations using subsystems technology. *BMC Genomics* **9:** 75.

Barry, T.N., Thompson, A., and Armstrong, D.G. (1977) Rumen fermentation studies on 2 contrasting diets.1. Some characteristics of invivo fermentation, with special reference to composition of gas-phase, oxidation-reduction state and volatile fatty-acid proportions. *J Agric Sci* **89:** 183–195.

Caporaso, J.G., Kuczynski, J., Stombaugh, J., Bittinger, K., Bushman, F.D., Costello, E.K., *et al*. (2010) QIIME allows analysis of high-throughput community sequencing data. *Nat Methods* **7:** 335–336.

Caporaso, J.G., Lauber, C.L., Walters, W.A., Berg-Lyons, D., Huntley, J., Fierer, N., *et al*. (2012) Ultra-high-throughput microbial community analysis on the Illumina HiSeq and MiSeq platforms. *ISME J* **6:** 1621–1624.

Daniel, J.L.P., Nussio, L.G., Amaral, R.C., Toledo, S.G., Lima, J.R., Cabezas, E., and Queiroz, O.C.M. (2010) Effect of the volatile fraction from silage and forage: concentrate ratio on ruminal degradation of fresh chopped or ensiled sugarcane. *J Dairy Sci* **93:** 152–152.

Danielsson, R., Schnurer, A., Arthurson, V., and Bertilsson, J. (2012) Methanogenic population and CH4 production in Swedish dairy cows fed different levels of forage. *Appl Environ Microbiol* **78:** 6172–6179.

David, L.A., Maurice, C.F., Carmody, R.N., Gootenberg, D.B., Button, J.E., Wolfe, B.E., *et al*. (2014) Diet rapidly and reproducibly alters the human gut microbiome. *Nature* **505:** 559–665.

Davis, L.M., Martinez, I., Walter, J., Goin, C., and Hutkins, R.W. (2011) Barcoded pyrosequencing reveals that consumption of galactooligosaccharides results in a highly specific bifidogenic response in humans. *PLoS One* **6:** e25200.

Faith, J.J., McNulty, N.P., Rey, F.E., and Gordon, J.I. (2011) Predicting a human gut microbiota's response to diet in gnotobiotic mice. *Science* **333:** 101–104.

Feillet-Coudray, C., Sutra, T., Fouret, G., Ramos, J., Wrutniak-Cabello, C., Cabello, G., *et al*. (2009) Oxidative stress in rats fed a high-fat high-sucrose diet and preventive effect of polyphenols: involvement of mitochondrial and NAD(P)H oxidase systems. *Free Radic Biol Med* **46:** 624–632.

Hammer, O. (2000) Spatial organization of tubercles and terrace lines in Paradoxides forchhammeri—evidence of lateral inhibition. *Acta Palaeontol Pol* **45:** 251–270.

Henderson, G., Cox, F., Ganesh, S., Jonker, A., Young, W., and Janssen, P.H. (2015) Rumen microbial community composition varies with diet and host, but a core microbiome is found across a wide geographical range. *Sci Rep* **5:** 14567.

Jami, E., Israel, A., Kotser, A., and Mizrahi, I. (2013) Exploring the bovine rumen bacterial community from birth to adulthood. *ISME J* **7:** 1069–1079.

Jonas, C.R., Estivariz, C.F., Jones, D.P., Gu, L.H., Wallace, T.M., Diaz, E.E., *et al*. (1999) Keratinocyte growth factor enhances glutathione redox state in rat intestinal mucosa during nutritional repletion. *J Nutr* **129:** 1278–1284.

Krishtalik, L.I. (2003) pH-dependent redox potential: how to use it correctly in the activation energy analysis. *Biochim Biophys Acta* **1604:** 13–21.

Ley, R.E., Hamady, M., Lozupone, C., Turnbaugh, P.J., Ramey, R.R., Bircher, J.S., *et al*. (2008) Evolution of mammals and their gut microbes. *Science* **320:** 1647–1651.

Liu, Q., Dong, C.S., Li, H.Q., Yang, W.Z., Jiang, J.B., Gao, W.J., *et al.* (2009) Effects of feeding sorghum-sudan, alfalfa hay and fresh alfalfa with concentrate on intake, first compartment stomach characteristics, digestibility, nitrogen balance and energy metabolism in alpacas (Lama pacos) at low altitude. *Livestock Sci* **126:** 21–27.

Lozupone, C.A., Stombaugh, J.I., Gordon, J.I., Jansson, J.K., and Knight, R. (2012) Diversity, stability and resilience of the human gut microbiota. *Nature* **489:** 220–230.

Mao, S.Y., Huo, W.J., and Zhu, W.Y. (2016) Microbiome-metabolome analysis reveals unhealthy alterations in the composition and metabolism of ruminal microbiota with increasing dietary grain in a goat model. *Environ Microbiol* **18:** 525–541.

Marounek, M., Bartos, S., and Kalachnyuk, G.I. (1982a) Dynamics of the redox potential and Rh of the Rumen fluid of goats. *Physiol Bohemoslov* **31:** 369–374.

Marounek, M., Bartos, S., and Kalachnyuk, G.I. (1982b) Dynamics of the redox potential and rh of the rumen fluid of goats. *Physiol Bohemoslov* **31:** 369–374.

Marounek, M., Roubal, P., and Bartos, S. (1987) The redox potential, rH and pH values in the gastrointestinal tract of small ruminants. *Physiol Bohemoslov* **36:** 71–74.

Muegge, B.D., Kuczynski, J., Knights, D., Clemente, J.C., Gonzalez, A., Fontana, L., *et al.* (2011) Diet drives convergence in gut microbiome functions across mammalian phylogeny and within humans. *Science* **332:** 970–974.

Quast, C., Pruesse, E., Yilmaz, P., Gerken, J., Schweer, T., Yarza, P., *et al.* (2013) The SILVA ribosomal RNA gene database project: improved data processing and web-based tools. *Nucleic Acids Res* **41:** D590–D596.

Saleem, F., Bouatra, S., Guo, A.C., Psychogios, N., Mandal, R., Dunn, S.M., *et al.* (2013) The bovine ruminal fluid metabolome. *Metabolomics* **9:** 360–378.

Shaver, R.D. (1997) Nutritional risk factors in the etiology of left displaced abomasum in dairy cows: a review. *J Dairy Sci* **80:** 2449–2453.

Walker, A.W., Duncan, S.H., McWilliam Leitch, E.C., Child, M.W., and Flint, H.J. (2005) pH and peptide supply can radically alter bacterial populations and short-chain fatty acid ratios within microbial communities from the human colon. *Appl Environ Microbiol* **71:** 3692–3700.

Walker, A.W., Ince, J., Duncan, S.H., Webster, L.M., Holtrop, G., Ze, X., *et al.* (2011) Dominant and diet-responsive groups of bacteria within the human colonic microbiota. *ISME J* **5:** 220–230.

Wright, J.J., Konwar, K.M., and Hallam, S.J. (2012) Microbial ecology of expanding oxygen minimum zones. *Nat Rev Microbiol* **10:** 381–394.

Xiao, Y., Cui, J., Shi, Y.H., Sun, J., Wang, Z.P., and Le, G.W. (2010) Effects of duodenal redox status on calcium absorption and related genes expression in high-fat diet-fed mice. *Nutrition* **26:** 1188–1194.

Yu, Y., Lee, C., Kim, J., and Hwang, S. (2005) Group-specific primer and probe sets to detect methanogenic communities using quantitative real-time polymerase chain reaction. *Biotechnol Bioeng* **89:** 670–679.

Yu, Z., and Morrison, M. (2004) Improved extraction of PCR-quality community DNA from digesta and fecal samples. *Biotechniques* **36:** 808–812.

Zerbino, D.R., and Birney, E. (2008) Velvet: algorithms for de novo short read assembly using de Bruijn graphs. *Genome Res* **18:** 821–829.

Zhou, M., Chung, Y.H., Beauchemin, K.A., Holtshausen, L., Oba, M., McAllister, T.A., and Guan, L.L. (2011) Relationship between rumen methanogens and methane production in dairy cows fed diets supplemented with a feed enzyme additive. *J Appl Microbiol* **111:** 1148–1158.

Supporting information

Additional Supporting Information may be found in the online version of this article at the publisher's web-site:

Fig. S1. Experimental design scheme. In the first experiment, which lasted 56 days, four cows were fed the high-grain diet for 31 days and then transferred to the non-grain diet for another 22 days, with a habituation period of 3 days (days 32–34). Each experimental diet consisted of a different proportion of the same dietary fiber in the feed. The first diet consisted of 65% grains (high-grain diet) and the second of 0% grains (non-grain diet). The second experiment performed with 5 cannulated Holstein Friesian cows, lasted for 69 days and divided into two feeding periods. During the first period, all cows were fed the non-grain diet for 39 days, and in the second period, which lasted 27 days, three cows were fed the high-grain diet while two cows remained on the non-grain diet as a control until the end of the experiment, to verify that environmental conditions did not affect the experimental results. A habituation period of 3 days (days 40–42) enabled a healthy change between the diets.

Fig. S2. Real-time qPCR of total archaea and the three major methanogenic orders - Methanobacteriales, Methanomicrobiales and Methanosarcinales. DNA was extracted from rumen samples and submitted to qRT-PCR analysis. The control group consisted of two cows maintained on a non-grain diet throughout the experiment. The experimental group consisted of three cows fed the different diets as follows: days 1-39, non-grain diet (light purple background); days 40-42, introduction period to new diet (dark gray background) and days 43-69, high-grain diet (light green). Each day represents the average of all cows within a group. The *X* axis represents day of the experiment. The *Y* axes of the three upper panels represent the proportion of each methanogen order out of total archaea. The *Y* axis in the lower panel represents the absolute archaeal 16S rRNA copy number. Mean for each time point is plotted ± SEM. Asterisks present significant differences (*t* test, $p < 0.05$) between the control and experimental group.

Table S1. Diets composition.